Chapter 2
Fire Modeling

2.1 Introduction

A real fire will generally undergo six stages which include ignition, growth, flashover, full fire development or steady burning, decay and extinguishment. Flashover is the rapid transition between the primary fire which is essentially localized around the item first ignited, and the general conflagration within the compartment when all fuel surfaces are burning [1]. Depending on whether flashover will happen or not, the real fires are usually divided into pre- and post-flashover fires. For small and middle scaled compartments with sufficient fuel and ventilation, the potential fires will develop to flashover and be characterized as post-flashover fires. For large scale enclosures or where sprinklers work effectively, flashover is unlikely to occur and the fires are characterized as pre-flashover fires. Post-flashover fires provide the worst case scenario which are usually considered in fire resistance design. However, localized heating of key elements of structure in pre-flashover fires must also be considered.

The behavior of a real fire is complex, which depends on many parameters such as active fire detection and suppression systems (smoke detector and sprinkler), fire load (amount and distribution), combustion, ventilation, compartment size and geometry, and thermal properties of compartment boundaries [2]. So far, with increase in complexity, empirical correlations (e.g. nominal fire curves and parameter fire curve [3]), zone models (e.g. one-zone models for post-flashover fires [4, 5] and two-zone models for pre-flashover fires [5, 6]), and sophisticated CFD models (e.g. Fire Dynamics Simulator [7]) have been developed to model the fire behavior. Also, stochastic models have been developed for compartment fires [8, 9].

In this chapter, the widely used one-zone model for modeling post-flashover fires is presented. Detailed description of the sub-models in one-zone model is given. A FE model is developed in ANSYS to simulate the one-zone model to give temperature-time curves for post-flashover fires. The concept of equivalent fire severity is also reviewed.

© Springer-Verlag Berlin Heidelberg 2015

C. Zhang, *Reliability of Steel Columns Protected by Intumescent Coatings Subjected to Natural Fires*, Springer Theses, DOI 10.1007/978-3-662-46379-6_2

2.2 One-Zone Compartment Fire Model

2.2.1 Heat Balance Equation

Figure 2.1 shows the widely used one-zone model for post-flashover fires. In this model, the heat balance equation within the compartment is given by [10]

$$HRR = \dot{q}_g + \dot{q}_w + \dot{q}_{o,c} + \dot{q}_{o,r} \tag{2.1}$$

where HRR is heat release rate due to combustion; $\dot{q}_g$ is rate of heat storage in the gas volume; $\dot{q}_w$ is rate of heat loss through the walls, ceiling and floor; $\dot{q}_{o,c}$ is rate of heat loss due to replacement of hot gases by cold; and $\dot{q}_{o,r}$ is rate of heat loss by radiation through the openings. Based on this model, both analytical expressions and compute programs have been developed to give fire curves for structural design [11].

2.2.2 Heat Release Rate (HRR)

Heat release rate (HRR) is the most important variable in measuring fire severity, which can be calculated by

$$HRR = \dot{m}_f \cdot \triangle H_c \tag{2.2}$$

where, $\dot{m}_f$ is the mass burning rate of the fuel; and $\triangle H_c$ is the net heat of combustion of the fuel. In ventilation controlled fires (fully-developed compartment or post-flashover fires), the HRRs can be alternatively calculated by [1]

$$HRR = \dot{m}_{air} \cdot \triangle H_{air} \tag{2.3}$$

where, $\dot{m}_{air}$ is the mass rate of air inflow and $\triangle H_{air}$ is the heat released per unit mass air consumed, for most common fuel, $\triangle H_{c,air} = 3.03 \pm 0.02$ MJ/kg [1].

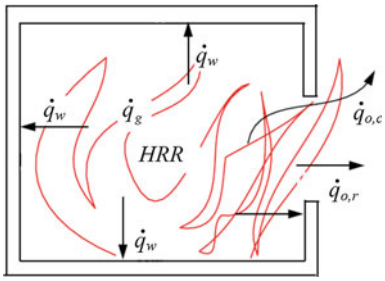


Fig. 2.1 Illustration of compartment one-zone model

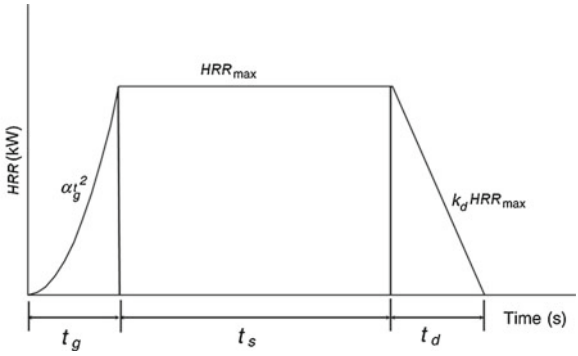


Fig. 2.2 Illustration of the *HRR* history in a NFSC fire

The *HRR* of a real fire can be measured by cone calorimeter [12]. In design work, the natural fire safety concept (NFSC) is widely used to represent the fire conditions [3, 5]. As shown in Fig. 2.2, the NFSC fire is assumed to be t-square in the growth stage and decay stage begins at the time when 70 % of design fire load is consumed. In a NFSC fire, at the growth stage, the *HRR* is given by

$$HRR = \alpha t^2 \tag{2.4}$$

the fire growth time t_g is given by

$$t_g = \sqrt{\frac{HRR_{\max}}{\alpha}} \tag{2.5}$$

and the fuel energy consumed at the fire growth stage, Q_g, is

$$Q_g = \int_0^{t_d} \alpha t^2 dt = \frac{\alpha {t_g}^3}{3} \tag{2.6}$$

where, α is the fire intensity coefficient, taken as 0.00293, 0.0117 and 0.0466 for slow, medium and fast growth fires, respectively.

The duration time of steady burning in a NSFC fire is given by

$$t_s = \frac{0.7 q_f A_f - Q_g}{HRR_{\max}} \tag{2.7}$$

and the duration of decaying stage is given by

$$t_d = \frac{0.6 q_f A_f}{HRR_{\max}} \tag{2.8}$$

where, q_f, A_f are design fire load density and floor area, respectively; and $HRR_{\max}$ is the maximum heat release rate, for ventilation controlled fires [1],

$$HRR_{\max} = 1{,}500 A_o \sqrt{H_o} \tag{2.9}$$

where, A_o is the total area of openings; and H_o is the weighted average of opening heights. For fuel-controlled fires, EC1 [3] gives some values of maximum heat release rates for different occupancies.

2.2.3 Heat Loss Due to Convective Flow ($\dot{q}_{o,c}$)

Pressure in a compartment fire is essentially atmospheric, and flows occur at openings due to hydrostatic pressure differences. The mass rates of out and in flows are calculated by [1]

$$\dot{m}_{gas} = \frac{2}{3} C_d W_o \rho_\infty [2g \frac{T_\infty}{T_g}(1 - \frac{T_\infty}{T_g})]^{1/2} (H_o - X_N)^{3/2} \tag{2.10}$$

and

$$\dot{m}_{air} = \frac{2}{3} C_d W_o \rho_\infty [2g(1 - \frac{T_\infty}{T_g})]^{1/2} (X_N - X_d)^{1/2} (X_N + X_d/2) \tag{2.11}$$

respectively. The heat loss due to replacement of hot gases by cold at openings is calculated by

$$\dot{q}_{o,c} = \dot{m}_{gas} c_p T_f - \dot{m}_{air} c_p T_\infty \tag{2.12}$$

The flow coefficient, C_d, is approximately 0.7. The neutral plane height, X_N, can be approximated as the half height of the opening. For post-flashover fires, the height of the interface X_d is approximately zero. Taken those values into Eq. 2.11, the inflow mass rate for post-flashover fires can be approximated as

$$\dot{m}_{air} = 0.5 A_o \sqrt{H_o} \tag{2.13}$$

In many calculations [1], the mass rate of outflow is taken as equal to the mass rate of inflow given by Eq. 2.13. Correspondingly, the heat loss due to replacement of hot gases by cold is calculated by

$$\dot{q}_{o,c} \approx 0.5 A_o \sqrt{H_o} c_p (T_f - T_\infty) \tag{2.14}$$

where, c_p is the specific heat of the gas; T_f and T_∞ are fire and environment temperatures, respectively.

2.2.4 Heat Loss by Radiation Through the Openings ($\dot{q}_{o,r}$)

The heat loss by radiation through the openings of a fire compartment is usually calculated by adopting homogeneous gray gas approximations for fire environment and using Stefan-Boltzmann law, that,

$$\dot{q}_{o,r} = A_o \varepsilon_f \sigma ({T_f}^4 - {T_\infty}^4) \tag{2.15}$$

where, ε_f is the effective emissivity of the gases within the compartment, which can be calculated from

$$\varepsilon_f = 1 - e^{-\kappa L} \tag{2.16}$$

where, κ is the extinction coefficient, usually taken as $1.1\,\mathrm{m}^{-1}$ [10]; and L is the mean beam length for the enclosure, which is approximated as the height of the compartment.

2.2.5 Heat Loss Through Wall ($\dot{q}_w$)

The heat transfer into the boundary surface of a compartment occurs by convection and radiation from the enclosure, and then conduction through the walls. In calculating heat transfer from fire to boundary surface ($\dot{q}_w$), the following assumptions are adopted,

- In radiation calculation, the fire and the boundary surface are represented as two infinitely parallel grey planes that the view factor is taken as unit;
- In unsteady conduction calculation, The boundaries (walls, ceiling and floor) are usually assumed to be semi-infinite solids.

Theoretically, for semi-infinite behavior, the exposure time must be less than the penetration time (which for a slab exposed to Dirichlet boundary condition is about $\frac{1}{\alpha_w}(\frac{\delta_w}{4})^2$ [1]). In practice, if the thickness of a slab is greater than $2\sqrt{\alpha_w t}$, the semi-infinite solid assumption is applicable [1, 13].

The governing equation for 1D wall conduction is given by

$$\frac{\partial^2 T_w(x,t)}{\partial x^2} = \frac{1}{\alpha_w}\frac{\partial T_w(x,t)}{\partial t} \tag{2.17}$$

where, $\alpha_w = k_w/(\rho_w c_w)$ is the thermal diffusivity of the wall. k_w, ρ_w and c_w are conductivity, density and specific heat of the wall, respectively.

At fire and environment exposed sides, the Neumann boundary conditions are given by

$$\dot{q}_w = -k_w \frac{\partial T_w(0,t)}{\partial x} = (h_{c,l} + h_{r,l})[T_f - T_w(0,t)] \tag{2.18}$$

and

$$-k_w \frac{\partial T_w(\delta_w, t)}{\partial x} = (h_{c,r} + h_{r,r})[T_w(\delta_w, t) - T_\infty], \tag{2.19}$$

respectively. Here, $T_w(0, t)$ and $T_w(\delta_w, t)$ are temperatures of fire and environment exposed surfaces, respectively; δ_w is the thickness of the wall; $h_{c,l}$ and $h_{c,r}$ are convective heat transfer coefficients at fire and environment exposed surfaces, taken as 35 and 9 W/m^{2}K [3], respectively; and $h_{r,l}$ and $h_{r,r}$ are radiative heat transfer coefficients at fire and environment exposed surfaces, given by

$$h_{r,l} = \varepsilon_{res}\sigma[(T_f + 273)^2 + (T_w(0, t) + 273)^2][T_f + 273 + T_w(0, t) + 273] \tag{2.20}$$

and

$$h_{r,r} = \varepsilon_w\sigma[(T_\infty + 273)^2 + (T_w(\delta_w, t) + 273)^2][T_\infty + 273 + T_w(\delta_w, t) + 273] \tag{2.21}$$

respectively. Here, ε_{res} is the resultant emissivity at fire exposed surface, given by

$$\varepsilon_{res} = \frac{1}{1/\varepsilon_f + 1/\varepsilon_w - 1} \tag{2.22}$$

in which, ε_w is the emissivity of the wall.

2.2.6 Heat Storage in Gas Volume ($\dot{q}_g$)

The heat stored in the gas volume within the compartment is calculated by

$$\dot{q}_g = \rho_\infty c_p V_g \frac{\Delta T_f}{\Delta t} \tag{2.23}$$

where, ρ_∞ is the density of the gas; and V_g is the gas volume.

2.3 Temperature-Time Curves for Post-Flashover Fires

2.3.1 Standard Fire

The ISO834 standard temperature-time curve is given by [3]

$$T_g = 20 + 345\log_{10}(8t + 1) \tag{2.24}$$

where, t is the standard fire exposure time in minutes.

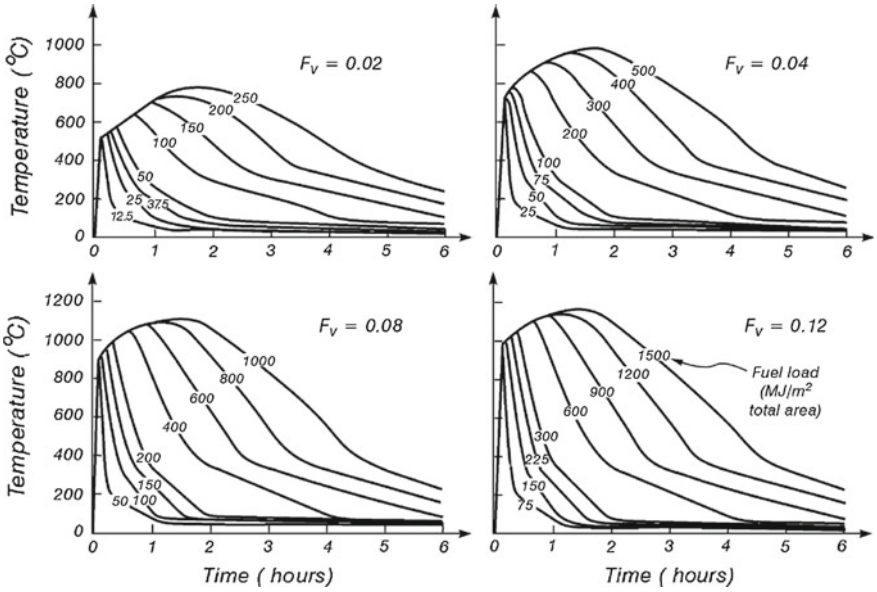


Fig. 2.3 Swedish *curves*

2.3.2 Swedish Curves

As shown in Fig. 2.3, the 'Swedish' fire curves are widely referenced in fire engineering. The 'Swedish' fire curves are derived by solving the heat balance equation for one-zone compartment fire model (see Eq. 2.1) with using the burning rate of ventilation controlled fires [10].

2.3.3 Lie Correlations

In SFPE handbook [14], correlations given by Lie are adopted for determining real fire temperatures. In the heating phase, the expression is given by

$$T_g = 250(10F_o)^{\frac{0.1}{F_o^{0.3}}} e^{-2F_o t}[3(1-e^{-0.6t}) - (1-e^{-3t}) + 4(1-e^{-12t})] + C(\frac{600}{F_o})^{0.5} \tag{2.25}$$

where, C is a constant taking into account the influence of the properties of the boundary material on the temperature. $C = 0$ for heavy materials ($\rho \geq 1{,}600\,\text{kg/m}^3$), and $C = 1$ for light materials ($\rho < 1{,}600\,\text{kg/m}^3$). F_o is the opening factor, defined by

$$F_o = \frac{A_o\sqrt{H_o}}{A_T} \tag{2.26}$$

Equation 2.25 is valid for

$$t \leq \frac{0.08}{F_o} + 1 \tag{2.27}$$

and

$$0.01 \leq F_o \leq 0.15. \tag{2.28}$$

If $t > 0.08/F_o + 1$, a value of $t = 0.08/F_o + 1$ should be used. If $F_o > 0.15$, a value of $F_o = 0.15$ should be used.

The duration of heating is determined by

$$\tau = \frac{q_{t,wood}}{330 F_o} \tag{2.29}$$

where, $q_{t,wood}$ is the wood equivalent fire load density, determined by

$$q_{t,wood} = \frac{q_f A_f}{A_t} \frac{1}{\triangle H_{c,wood}} \tag{2.30}$$

here, A_t is the area of bounding surfaces, taken as the total enclosure area in post-flashover fires; and $\triangle H_{c,wood}$ is the net calorific value of wood, often taken as 17.5 MJ/kg [3].

In the cooling phases, the fire temperature is calculated by

$$T_g = -600(\frac{t}{\tau} - 1) + T_\tau \geq 20\,^\circ\mathrm{C} \tag{2.31}$$

2.3.4 EC1 Parameter Fire Curve

In EC1 [3], the parameter fire model developed by Wickstrőm is adopted for calculation in real fires. In the heating phase, the fire temperature is

$$T_g = 20 + 1{,}325(1 - 0.324e^{-0.2t^*} - 0.204e^{-1.7t^*} - 0.472e^{-19t^*}) \tag{2.32}$$

where, $t^* = t\Gamma$, in which

$$\Gamma = \frac{(F_o/\sqrt{k\rho c})^2}{(0.04/1{,}160)^2}. \tag{2.33}$$

$\sqrt{k\rho c}$ is the thermal inert of the enclosure.

The duration of the heating is determined by

$$t_{\max} = \max\left(\frac{0.2 \times 10^{-3} q_t}{F_o}, t_{lim}\right) \tag{2.34}$$

where, $t_{lim} = 25$, 20 and 15 min for slow, medium and fast fires, respectively. If $t_{\max} = 0.2 \times 10^{-3} q_t / F_o$, the fire is ventilation controlled; and if $t_{\max} = t_{lim}$, the fire is fuel controlled. For fuel controlled fires, when using Eq. 2.33 to calculate Γ_{lim}, $F_{o,lim}$ is taken as $0.1 \times 10^{-3} q_t / t_{lim}$.

Equation 2.32 is valid for

$$100 \leq \sqrt{k\rho c} \leq 2{,}200 \tag{2.35}$$

and

$$0.02 \leq F_o \leq 0.20 \tag{2.36}$$

In the cooling phases, the fire temperature is calculated by

$$T_g = T_{\max} - 625(t^* - t^*_{\max} \cdot x) \quad (t^*_{\max} \leq 0.5) \tag{2.37a}$$

$$T_g = T_{\max} - 250(3 - t^*_{\max})(t^* - t^*_{\max} \cdot x) \quad (0.5 < t^*_{\max} \leq 2) \tag{2.37b}$$

$$T_g = T_{\max} - 250(t^* - t^*_{\max} \cdot x) \quad (t^*_{\max} \geq 2) \tag{2.37c}$$

where, $t^*_{\max} = (0.2 \times 10^{-3} q_t / F_o)\Gamma$. For $t_{\max} > t_{lim}$, x=1; and for $t_{\max} = t_{lim}$, $x = t_{lim}\Gamma / t^*_{\max}$.

Lie correlations are only applicable for ventilation controlled fires, whilst EC1 correlations are applicable for both ventilation and fuel controlled fires. For ventilation controlled fires, the duration of the heating calculated by Lie and EC1 correlations are equal, thus

$$\tau = \frac{q_t A_t}{\dot{m}_{air} \triangle H_{c,air}} = \frac{q_t A_t}{0.52 A_o \sqrt{H_o} \times 3.03 \times 3{,}600} \approx \frac{0.2 \times 10^{-3} q_t}{F_o} \tag{2.38}$$

$$= \frac{17.5 q_{t,wood} A_t}{0.52 A_o \sqrt{H_o} \times 3.03 \times 3{,}600} \approx \frac{q_{t,wood}}{330 F_o} \tag{2.39}$$

2.4 The Concept of Time Equivalent

2.4.1 Overview

The concept of equivalent fire severity, commonly referred as time equivalent, is used to relate the severity of an expected real fire to the standard fire. So that results or methods based on standard fire can be extended to realistic fires. The concept was

originally developed by Ingberg [15]. Till now, a number of methods and empirical formulae have been developed for evaluating the equivalent fire severity. These methods include equal area method, maximum temperature method, minimum load capacity concept and energy based method [11, 16, 17].

Equal area method establishes time equivalency by equating the area under the time-temperature curve of design fire scenario to that under the standard fire scenario. If the areas under different curves are equal, the fires are considered to have equivalent severity. This method has no rational basis and might underestimate the heat transfer in a short hot fire and overestimate the heat transfer in a long cold fire, although both result in equal areas under two time-temperature curves [11].

Maximum temperature method defines the equivalent fire severity as the time of exposure to the standard fire that would result in the same maximum temperature in a protected steel member as would occur in a realistic fire. This method is the most widely used time equivalent concept. The empirical formulae for evaluating the equivalent fire severity, such as CIB, Law and Eurocode formulae [11], are based on this method. This method may not be accurate if the maximum temperatures used for computing the time equivalent are much higher or lower than those which would cause failure in a particular member.

Minimum load capacity method establishes the equivalent fire severity as the time of exposure to the standard fire that would result in the same load bearing capacity as the minimum which would occur in a realistic fire. This method is the most realistic time equivalent concept for the design of load bearing members, but it is difficult to implement for a material which does not have a clearly defined minimum load capacity.

The energy based method establishes the equivalency to the amount of energy transferred to the elements. Two fires will have the same fire severity if they transfer same amount of energy to an element. The method is originally proposed by Harmathy [16]. Harmathy [16] introduced a variable referred to as 'normalized heat load' to calculate the amount of the energy. The normalized heat load is defined as the total heat absorbed by a unit area of the boundaries of an enclosure during any fire, divided by the thermal absorptivity of the boundaries. The normalized heat load is the measure of the maximum temperature rise below the surface of a building element at a depth corresponding roughly to a distance where the important load-bearing components (e.g. steel bars) are located [17]. Recently, the energy based method has been adopted by Kodur et al. [17] to evaluate fire resistance of reinforced concrete beams.

2.4.2 EC1 Correlation

The Eurocode formula [3], based on maximum temperature method, is used to calculate the equivalent standard fire duration of natural fires. The formula is based on maximum temperature method which is derived for protected steel members.

Compare with other formulae based on maximum temperature method, the Eurocode formula is presented in a very simple form given by

$$t_{eq} = q_f k_b w_f \tag{2.40}$$

where, t_{eq} is the equivalent standard fire duration time in minutes; q_f is the floor fire load density; k_b is the conversion factor to account for the thermal properties of the enclosure; and w_f is the ventilation factor, for small compartments without horizontal vents

$$w_f = (\frac{A_o\sqrt{H_o}}{A_t})^{-1/2}\frac{A_f}{A_t} = {F_o}^{-1/2}\frac{A_f}{A_t} \tag{2.41}$$

2.5 Finite Element Simulation

2.5.1 Numerical Tool

The one-zone compartment fire model given above can be solved using technologies like finite differential method (FDM) and finite element method (FEM). In this section, the FEM program ANSYS is employed to simulate the model. ANSYS is power to solve steady-state or transient heat transfer problems, it capacity for using in fire environment has been validated by many works, e.g. [18, 19].

2.5.2 Basic Elements

2.5.2.1 LINK32-2D Conduction Bar

LINK32 is a uniaxial element with the ability to conduct heat between its nodes. The element has a single degree of freedom, temperature, at each node point. The conducting bar is applicable to a 2D, steady-state or transient thermal analysis.

The element is defined by two nodes, a cross-sectional area, and the material properties. The thermal conductivity is in the element longitudinal direction. Heat generation rates may be input as element body loads at the nodes.

2.5.2.2 LINK34-Convection Link

LINK34 is a uniaxial element with the ability to convect heat between its nodes. The element has a single degree of freedom, temperature, at each node point. The convection element is applicable to a 2D or 3D, steady-state or transient thermal analysis.

The element is defined by two nodes, a convection surface area, two empirical terms, and a film coefficient.

2.5.2.3 LINK31-Radiation Link

LINK31 is a uniaxial element which models the radiation heat flow rate between two points in space. The link has a single degree of freedom, temperature, at each node. The radiation element is applicable to a 2D or 3D, steady-state or transient thermal analysis.

The element is defined by two nodes, a radiating surface area, a geometric form factor, the emissivity, and the Stefan-Boltzmann constant.

2.5.2.4 MASS71-Thermal Mass

MASS71 is a point element having one degree of freedom, temperature, at the node. The element may be used in a transient thermal analysis to represent a body having thermal capacitance capability but negligible internal thermal resistance, that is, no significant temperature gradients within the body. The lumped thermal mass element is applicable to a 1-D, 2-D, or 3-D steady-state or transient thermal analysis.

The lumped thermal mass element is defined by one node and a thermal capacitance.

2.5.3 FE Model

Figure 2.4 illustrates the FE model. The heat source is modeled by a perfect conductor, which is represented by one LINK32 element. The heat generation rate of the source is input as *HRR* specified by NFSC. The compartment boundaries are modeled using LINK32. Convection and radiation at fire or environment exposed surfaces are

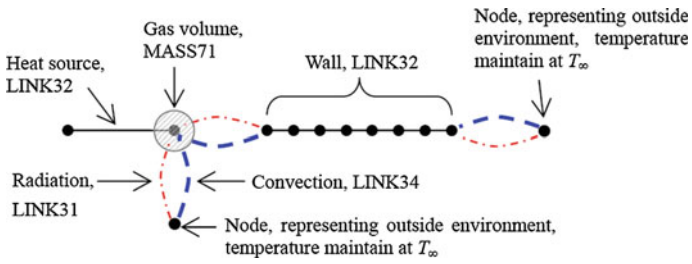


Fig. 2.4 FE Model for one zone compartment fire model

modeled using LINK34 and LINK31, respectively. Gas volume is modeled using MASS71. Radiation at opening is modeled using LINK31. Convection at opening by mass exchange is modeled using LINK34 with film coefficient of $c_p \dot{m}_{gas}/A_o$.

2.5.4 Verification of the FE Model

The results for fire temperatures predicted by the proposed model simulated by FEM are compared with those predicted by the program OZone [5], Lie correlations [14] and EC1 parameter fire model [3]. The program OZone V2 was developed by Cadorin et al. [5] to design structural steel elements submitted to compartment fires. In OZone V2, both two- and one-zone models are adopted to simulate the pre- and post-flashover fires. Under certain circumstances, the two-zone model can also switch automatically to a one-zone model.

In the study, $W \times D \times H = 3\,\text{m} \times 3\,\text{m} \times 2\,\text{m}$, $W_o \times H_o = 2\,\text{m} \times 1\,\text{m}$, $d_w = 0.2\,\text{m}$, $\rho_w = 2{,}300\,\text{kg/m}^3$, $c_w = 1{,}000\,\text{J/(kgK)}$, $k_w = 1.6\,\text{W/mK}$, $q_f = 800\,\text{MJ/m}^2$, $\alpha = 0.0117$, and the maximum heat release rate per unit area for fuel controlled fire is taken as $250\,\text{kW/m}^2$. Correspondingly, the calculated $HRR_{\max}$ for fuel and ventilation controlled fires are 2.25 and 3.0 MW respectively.

Figure 2.5 shows the comparison among the results of fire temperatures predicted by different methods. The FEM model and Ozone give consistent results for both fuel ($HRR_{\max} = 2.25\,\text{MW}$) and ventilation ($HRR_{\max} = 3\,\text{MW}$) controlled fires, whilst in the heating phases the fire temperatures predicted by the FEM model are slightly higher than those predicted by Ozone. The differences among the results by FEM model and Ozone are due to different mathematic technologies adopted by them in solving sub-models in one zone post-flashover fire model [5]. Results by Lie method agree well with those by FEM model using $HRR_{\max} = 2.25\,\text{MW}$ in the heating phases. Lie method and EC1 parameter fire give same results for fuel and ventilation controlled fires.

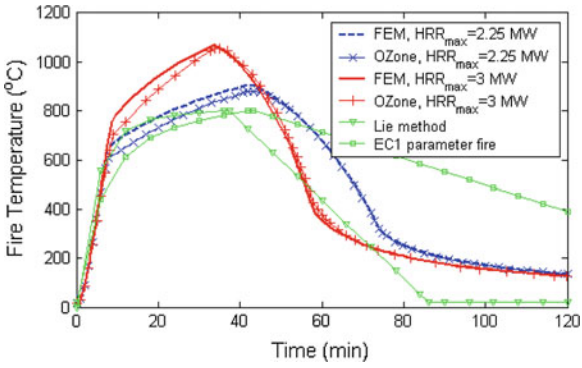


Fig. 2.5 Comparison among results of fire temperatures predicted by different methods

2.6 Conclusion

The widely used one-zone model for post-flashover fires has been presented. Based on the one-zone model, a FE model is developed to simulate the post-flashover fires. The FE model has been verified, which will be used in the following chapter.

References

1. D. Drysdale, *An Introduction to Fire Dynamics*, 2nd edn. (Wiley, New York, 1999)
2. J. Quintiere, *Fundamentals of Fire Phenomena* (Wiley, New York, 2006)
3. BSI, *Eurocode 1: Actions on Structures—Part 1–2: General Rules—Actions on Structures Exposed to Fire* (British Standard, UK, 2002)
4. V. Babrauskas, Compf2: a program for claculating post-flashover fire temperatures. Technical report, NBS Technical Note 991. National Bureau of Standards (1979)
5. J. Cadorin, J. Franssen, Fire Saf. J. **38**, 395 (2003)
6. W. Jones, R. Peacock, G. Forney, P. Reneke, Cfast—consolidated model of fire growth and smoke transport (version 6): Technical reference guide. Technical report, NIST Special Publication 1026, National Institude of Standard and Technology (NIST) (2009)
7. K. McGrattan, R. McDermott, S. Hostikka, J. Floyd, Fire dynamics simulator (version 5) user's guide. Technical report, NIST Special Publication 1019-5, NIST (2010)
8. A. Hasofer, V. Beck, Fire Saf. J. **28**, 207 (1997)
9. V. Bertola, E. Cafaro, Proc. R. Soc. A **465**, 1029 (2009)
10. O. Pettersson, S. Magnusson, J. Thor, *Fire Engineering Design of Steel Structures* (Swedish Institute of Steel Construction, Sweden, 1976)
11. A. Buchanan, *Structural Design for Fire Safety* (Wiley, New York, 2001)
12. V. Babrauskas, *SFPE Handbook of Fire Protection Engineering*, 3rd edn. (Society of Fire Protection Engineers, 2002), chap. Section 3–1: Heat Release Rates
13. B. McCaffrey, J. Quintiere, M. Harkleroad, Fire Technol. **17**(2), 98 (1981)
14. T. Lie, *SFPE Handbbok of Fire Protection Engineering*, 3rd edn. (Society of Fire Protection Engineers, 2002), chap. Section 4–8: Fire Temperature-Time Relations
15. S. Ingberg, NFPA Q. **22**, 43 (1928)
16. T. Harmathy, Fire and Mater. **11**, 95 (1987)
17. V. Kodur, P. Pakala, M. Dwaikat, Fire Saf. J. **45**, 211 (2010)
18. G. Li, C. Zhang, Int. J. Adv. Steel Constr. **6**(2), 788 (2010)
19. C. Zhang, G. Li, Y. Wang, Fire Technol. (2011)

http://www.springer.com/978-3-662-46378-9

Reliability of Steel Columns Protected by Intumescent Coatings Subjected to Natural Fires

Zhang, C.

2015, XXIV, 140 p. 74 illus., Hardcover
ISBN: 978-3-662-46378-9